Magnetic Double Resonance in Force Microscopy

Qiong Lin, Christian L. Degen, Marco Tomaselli, Andreas Hunkeler, Urban Meier, and Beat H. Meier*

Physical Chemistry, ETH Zurich, CH-8093 Zurich, Switzerland

(Received 15 December 2005; published 7 April 2006)

Magnetic-resonance force microscopy is combined with cross-polarization and spin-decoupling NMR techniques to obtain double-resonance NMR signals of micrometer-scaled objects. The effective one-dimensional spatial resolution obtained in our experiments performed on a KPF_6 single crystal sample is $\sim 0.5\ \mu$m. The spectral linewidth of 900 Hz is sample limited. The described double-resonance techniques can introduce new chemical specificity to the magnetic-force sensor.

DOI: 10.1103/PhysRevLett.96.137604 PACS numbers: 76.70.−r, 68.37.Rt, 76.60.Lz, 76.60.Pc

Conventional localized magnetic-resonance spectroscopy combines magnetic-resonance imaging techniques with magnetic-resonance spectroscopy (NMR). The method is noninvasive and can physicochemically characterize materials with a spatial resolution down to roughly a hundred micrometers. The limit to spatial resolution is given by the detection sensitivity and the magnitude of the field gradient: using inductive methods, the number of spins in a volume element should exceed 10^{12} for single-resonance and more for double-resonance spectroscopy. Recently, it has been demonstrated that magnetic-resonance force detection (MRFM) [1–3] can be combined with NMR spectroscopy to extend localized spectroscopy of solid materials to the micrometer and nanometer scale [4]. While these experiments were limited to one spectral and spatial dimension only, extension to three spatial dimensions [2,5] and to more spectral dimensions [6–8] is obvious. The sensitivity limits for MRFM of nuclear spins are still being explored, but as few as 10^8 nuclear spins (10^4 net spins) have been detected at low temperature [9]. To spatially resolve two volume elements, the difference in resonance frequency induced by the field gradient must exceed the spectral line width. Field gradients in MRFM can exceed 10^5 T/m and allow for nanometer spatial resolution even in compounds with inherently broad NMR lines [10].

The setup for nanoscale localized spectroscopy follows the general scheme of multidimensional NMR spectroscopy [8]. The spectral information is sampled in an indirect dimension point by point. The direct dimension contains spatial information, namely, slice selection and signal intensity are proportional to the number of spins in the slice. The slice geometry is given by the position and shape of the gradient magnet, and the slice thickness can be chosen by the depth of the adiabatic modulation during mechanical readout. Would it not be for the large field gradient needed for sensitive force detection, the wide range of solid-state NMR techniques available today could directly be applied in the indirect dimensions of the MRFM experiment. The presence of the gradient still interferes with spectral resolution in many cases, but dipolar spectroscopy at high resolution has been demonstrated [4] and quadrupolar interactions have also been used for chemical specificity in the context of nutation spectroscopy [11].

Double- and multiple-resonance spectroscopy is a key technology in modern NMR spectroscopy [8] and is of great importance, in particular, in cases where the spectral resolution is limited. It is not only possible to use the spectral parameters of both spin types for chemical characterization of the sample but, in addition, the atomic connectivities and interatomic distances can be probed using heteronuclear correlation spectroscopy [8] (HETCOR). In this Letter we demonstrate MDRFM (magnetic double-resonance in force microscopy) with two basic double-resonance experiments using a home-built magnetic-resonance force microscope [see Fig. 1]: Hartmann-Hahn cross polarization (CP) [12,13], leading to polarization transfer between two spin species, and spin decoupling, leading to line narrowing due to the averaging of the heteronuclear spin-spin interactions. Cross polarization in the rotating frame [12,14] is regularly used in NMR to enhance the spin polarization of nuclei with low magnetogyric ratio and for HETCOR experiments. The transfer of

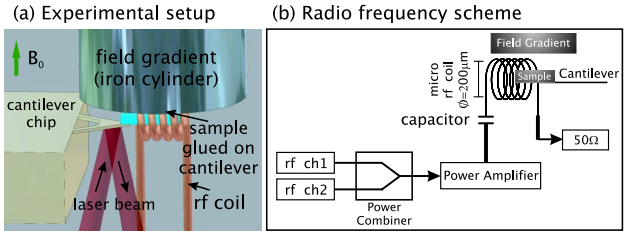

FIG. 1 (color online). (a) Experimental setup: The MDRFM probe assembly operates in a 89 mm-bore NMR magnet. A small iron cylinder is placed close to a micron-sized KPF_6 sample, which is glued onto a cantilever tip. The 4 turn, 200 μm inner diameter coil was made of 50 μm thick copper wire. (b) Radio frequency scheme: The rf pulses for the two channels are generated separately, fed through a power combiner, and amplified. The rf circuit is broadband (see text).

polarization between two nuclear spin species is accomplished by the simultaneous irradiation with two resonant rf fields. Decoupling techniques are widely used for narrowing resonance lines [15].

The experiments were performed on a set of two KPF_6 crystals with dimensions of $80 \times 40 \times 45$ μm^3 and $60 \times 30 \times 45$ μm^3 glued to the tip of a commercially available silicon nitrite cantilever (Veeco Instruments, $k = 0.01$ N/m, $f_c = 841$ Hz, and $Q = 11\,000$). The total sample consists of 7.2×10^{15} ^{19}F and 1.2×10^{15} ^{31}P spins, respectively. In our setup [Fig. 1(a)], we adapted a sample-on-cantilever design as described by Rugar *et al.* [16].

The MDRFM probe operated at room temperature and at $\sim 10^{-5}$ mbar fits into a widebore 5.87 T NMR magnet (Oxford). We use an iron cylinder as the gradient source (0.5 mm diameter, 10 mm length, $B_{sat} = 1.75$ T) which can be positioned close to the sample by means of a home-built *x, y, z*-piezo system. The cantilever vibration is detected with a deflected laser beam and analyzed using a position-sensitive photodiode connected to a lock-in amplifier (SR830, Stanford Research). Feedback control is applied to an additional piezo attached to the base of the cantilever which increases the bandwidth and keeps the cantilever damping time acceptably low [17,18]. Figure 1(b) shows the MRFM spectrometer scheme used in the double-resonance experiments. The rf pulses of the ^{31}P channel (ch1) are generated by an arbitrary waveform generator (NI-5411, National Instruments) and mixed with the intermediate frequency of a PTS-300 rf synthesizer (Programmed Test Sources, Inc.). The rf of the ^{19}F channel (ch2) is generated by a second synthesizer and fed into a home-built quadrature phase shifter. Both ^{31}P and ^{19}F rf signals, gated by the pulse program, are fed into a power combiner (PSC2-1, Minicircuit) and amplified by a single Blax1000 (Bruker BioSpin) power stage. Semirigid coaxial lines (50 Ω) are used to transmit the rf pulses to the rf circuit of the MDRFM probe and a 50 Ω external load. The rf circuit with a 56 pF series matching capacitor is broadband enough to support both rf frequencies, $\omega_0^F/2\pi = 256$ MHz and $\omega_0^P/2\pi = 109$ MHz.

Figure 2(a) shows the MDRFM radio frequency scheme. The thermal polarization of the ^{19}F nuclei is transferred to the ^{31}P nuclei using a Hartmann-Hahn experiment with an additional rf-amplitude sweep of the ^{31}P channel [19]. Efficient transfer requires that the Hartmann-Hahn condition $\omega_{eff}^F = \omega_{eff}^P$ is fulfilled, where $\omega_{eff}^F = \sqrt{(\omega_1^F)^2 + (\Omega^F)^2}$, and $\omega_{eff}^P = \sqrt{(\omega_1^P)^2 + (\Omega^P)^2}$. The resonance offsets Ω^F and Ω^P denote the frequency differences between the rf-irradiation frequencies ω_{rf}^F, ω_{rf}^P and the Larmor frequencies $\omega_0^F = -\gamma_F B_0$, $\omega_0^P = -\gamma_P B_0$, respectively, and ω_1^F and ω_1^P describe the respective rf-field amplitudes (in units of angular frequency). NMR experiments in homogeneous magnetic field are best performed with on-resonance irradiation ($\Omega^F = \Omega^P = 0$). As a consequence of the strong field gradient in the MRFM experiment, the on-resonance condition can be satisfied only in a central slice where the resonance offsets Ω^F and Ω^P are both close to zero (vide infra). The offsets are related by the ratio of the magnetogyric ratios, $\Omega^F = (\gamma_F/\gamma_P)\Omega^P$. Efficient polarization transfer occurs as long as $\omega_{eff}^F - \omega_{eff}^P$ is smaller than the ^{19}F linewidth. Because of the free rotation of the PF_6^- groups in the crystal, all intragroup dipolar interactions are averaged to zero and the second moment of the fluorine resonance is relatively small ($\sqrt{M_2} = 4.1$ kHz) [20]. This offset effect limits the sensitive slice to a fraction of a μm in the present experiments and leads to a signal-to-noise ratio barely detectable in the present setup. It should be noted that, for systems with larger dipolar interactions, the sensitive slice would be correspondingly thicker. The most efficient scheme to experimentally broaden the sensitive slice is the application of a frequency sweep to both rf channels such that the rf-irradiation frequency during the CP pulses is given by $\omega_{rf}^P(t) = (t/\tau_{CP} - 1/2)\Delta\Omega^P + \omega_0^P$ and $\omega_{rf}^F = (\gamma_F/\gamma_P)\omega_{rf}^P$, where τ_{CP} is the CP contact time and $\Delta\Omega^P$

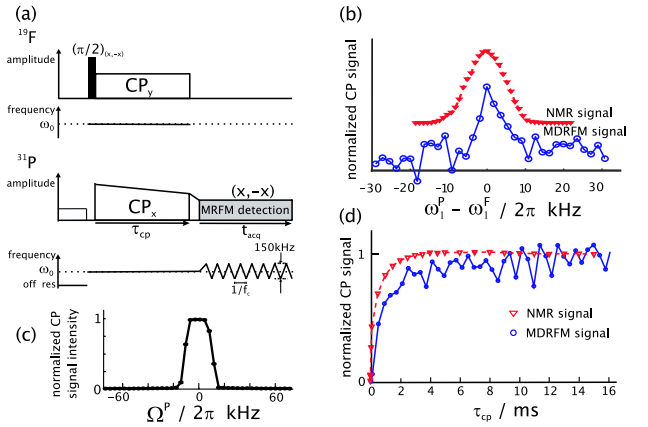

FIG. 2 (color online). (a) MDRFM-CP pulse scheme in KPF_6: an amplitude modulation on the ^{31}P channel is used during the polarization transfer step (CP contact time). After the CP step the ^{31}P rf amplitude is swept down to ~15 kHz for the adiabatic inversion cycle for detection. The phase cycle eliminates the disturbance from rf-cantilever couplings. (b) CP matching profiles in KPF_6 at $\omega_1^F/2\pi = 50$ kHz for the MDRFM-CP experiment and a conventional NMR-CP experiment performed in at a magnetic field of 11.75 T. The MDRFM-CP contact time was 10 ms in both cases. Two-hundred experimental cycles were averaged for the MDRFM in order to achieve a signal-to-noise ratio of ~6 (measurement time ~40 min per point) [23]. (c) $^{19}F \rightarrow {}^{31}P$ CP efficiency depending on the ^{31}P resonance offset recorded in a conventional NMR-CP experiment. The ^{19}F offset was larger by the ratio of the magnetogyrotic ratios to simulate the offset encountered in the MDRFM experiment [$\Omega^F = (\gamma_F/\gamma_P)\Omega^P$, $\omega_1^F/2\pi = 50$ kHz and $\omega_1^P/2\pi = 50$ kHz, and $\Delta\omega_1^P = 3.5$ kHz]. (d) CP buildup curve of the ^{31}P magnetization signal in KPF_6 in an MDRFM experiment ($\omega_1^F/2\pi = 50$ kHz and $\omega_1^P/2\pi = 50$ kHz and $\Delta\omega_1^P = 3.5$ kHz) and in a conventional on-resonance NMR experiment ($\omega_1^F/2\pi = 50$ kHz and $\omega_1^P/2\pi = 50$ kHz).

characterizes the width of the frequency ramp. For such an irradiation scheme, each resonance slice within the range $\omega_0^P - \Delta\Omega^P/2$ and $\omega_0^P + \Delta\Omega^P/2$ passes through the exact Hartmann-Hahn condition at some time during the frequency sweep. Our present setup does, however, support only a fixed rf-irradiation frequency on the ^{19}F channel. Therefore, we have resorted to an alternative scheme to broaden the Hartmann-Hahn condition. Keeping the rf frequencies on both channels fixed, we have modulated the rf amplitude on the ^{31}P channel, ω_1^P, in a linear ramp with variation $\Delta\omega_1^P$ and average amplitude ω_1^P: $\omega_1^P(t) = (t/\tau_{CP} - 1/2)\Delta\omega_1^P + \omega_1^P$. This scheme also leads to a sequential match of resonance slices during the ramp. In contrast to the frequency modulation scheme where the size of the heteronuclear coupling element b responsible for transfer is identical for all resonance slices, the amplitude variation leads to an offset-dependent effective coupling element of $b_{eff} = b\Omega^F\Omega^P/\omega_{eff}^F\omega_{eff}^P \leq b$. This variation is caused by the fact that the two effective fields are oriented at an angle at the Hartmann-Hahn matching condition.

In all CP experiments described here, the ^{19}F spins were locked in the rotating frame by a rf field of amplitude $\omega_1^F/2\pi = 50$ kHz, while on the ^{31}P channel a linear amplitude ramp with $\omega_1^P/2\pi = 50$ kHz and $\Delta\omega_1^P = 3.5$ kHz was used for polarization transfer [21]. MRFM detection employed adiabatic inversion cycles with a triangular frequency modulation with a depth of 150 kHz, an amplitude of $\omega_1^P/2\pi = 15$ kHz, and a cycle time adjusted to the inverse of the cantilever eigenfrequency (841 Hz). To transfer the magnetization present at the end of the CP period to the detection period, a linear amplitude ramp was employed. With a field gradient of 2.6×10^3 T/m a readout detection-slice thickness of 3.5 μm is obtained. Before each experiment, the ^{31}P spins were irradiated 300 kHz off resonance. This irradiation does not significantly affect the spins but has approximately the same dielectric heating effect on the cantilever as on-resonance irradiation and, therefore, avoids a strong step response of the cantilever to the CP rf pulse train which would interfere with signal detection.

Figure 2(b) shows the MDRFM-CP matching profile (transferred polarization as a function of the difference in rf-field amplitude) in KPF_6. The maximum of the curve corresponds to the Hartmann-Hahn condition. For comparison, a CP matching profile was recorded with conventional NMR in a homogeneous field $B_0 = 11.75$ T with a Varian Infinity 500 NMR spectrometer using a CP contact time $\tau_{CP} = 10$ ms. The width of the matching profile is similar in both cases and depends on the depth of the amplitude sweep, $\Delta\omega_1^P$. Note that all intramolecular ^{19}F-^{19}F and ^{31}P-^{19}F dipolar interactions are averaged to zero due to the rotation of the PF_6^- group, leading to a rather narrow matching profile. As discussed above, the strong field gradient of the MRFM experiments allows only spins in the center of the selected readout slice to be on resonance and to have efficient polarization transfer. To estimate the width of the sensitive slice, a series of conventional CP experiments was recorded. At constant, homogeneous B_0 field, the CP transfer efficiency was measured as function of the resonance offset Ω^P, while Ω^F was varied accordingly to ensure $\Omega^F = (\gamma_F/\gamma_P)\Omega^P$. The range of offsets covered corresponds to the readout slice in MDRFM detection. The results in Fig. 2(c) indicate that, outside a slice of thickness ~22 kHz, polarization transfer becomes very inefficient. Therefore, we can estimate the effective MDRFM-CP detection slice to be 0.5 μm thick and to contain about 4×10^{12} ^{31}P spins. The $^{19}F \rightarrow {}^{31}P$ CP buildup curve at $\omega_1^F/2\pi = 50$ kHz is shown in Fig. 2(d). The MDRFM polarization buildup rate is somewhat slower than in the conventional NMR experiment, due to the scaling of the effective dipolar interaction b_{eff} (note that the MDRFM-CP buildup is a superposition of CP transfer curves from spin packets with different resonance offset) [22].

In a second set of experiments the ^{31}P spectral linewidth under ^{19}F decoupling conditions was investigated with an MRFM-detected Hahn echo [4]. Figure 3(b) shows the MRFM and NMR ^{31}P spectra with ^{19}F decoupling by a 180° refocusing pulse on the ^{31}P channel.

The MRFM spin-echo spectrum has a linewidth of ~1.4 kHz [full width at half height (FWHH)], comparable to the ~1.2 kHz obtained in the conventional spin-echo NMR spectrum. The conventional single-pulse spectrum without decoupling has a FWHH of ~2.9 kHz. This shows that a partial line narrowing can be achieved by the spin-echo experiment which refocuses heteronuclear dipolar couplings as well as B_0 field inhomogeneity, ^{31}P chemical-shift dispersion, and bulk susceptibility effects. It is, however, known that decoupling by a 180° pulse is not very efficient in the presence of homonuclear ^{19}F-^{19}F interactions [15]. Further line narrowing can, therefore, be achieved by continuous wave ^{19}F decoupling as shown in Fig. 3(c). Here, the spin-echo MDRFM ^{31}P spectrum shows a linewidth of ~900 Hz. Further narrowing is observed when the spin echo is combined with CW decoupling where a FWHH ~ 820 Hz is found. The relatively modest improvement of CW decoupling over Hahn-echo decoupling is explained by the small size and particular form of the interaction in the presence of molecular motion [20].

In summary, we have shown that nuclear double-resonance experiments in a high magnetic field gradient can be successfully performed in combination with magnetic-resonance force detection. MDRFM cross-polarization and heteronuclear decoupling schemes are described. The advantage of the force-detection technique is its high sensitivity combined with the inherently high spatial resolution. The present experiments produce double-resonance spectra from 10^{12} to 10^{13} spins at room

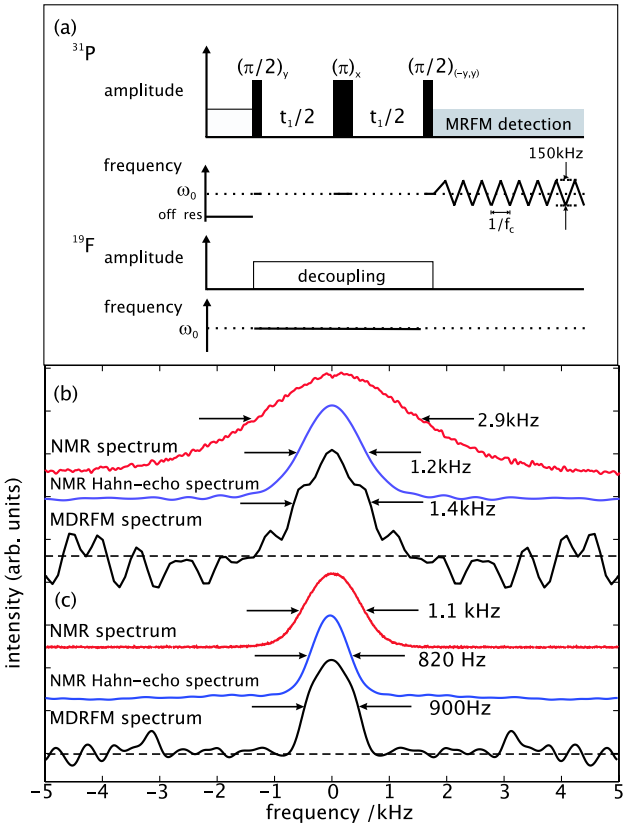

FIG. 3 (color online). ^{31}P spectra with and without ^{19}F decoupling. The MDRFM experiments are performed on a set of two KPF_6 single crystals, the conventional NMR experiments on KPF_6 powder. (a) MDRFM decoupling pulse scheme. (b) Spectra without ^{19}F irradiation. The MRFM ^{31}P Hahn-echo spectrum has a FWHH $\sim$ 1.4 kHz comparable to the conventional Hahn-echo NMR spectrum (FWHH $\sim$ 1.2 kHz) and narrower than the conventional one-pulse NMR spectrum (FWHH $\sim$ 2.9 kHz). (c) Spectra with 80 kHz ^{19}F cw irradiation. The MDRFM narrows to a FWHH $\sim$ 900 Hz, comparable to the conventional Hahn-echo NMR spectrum (FWHH $\sim$ 820 Hz) and narrower than the one-pulse spectrum (FWHH $\sim$ 1.1 kHz).

temperature, but further sensitivity improvements are realistic. MDRFM opens new avenues by adding chemical specificity to the MRFM method with the possibility to interrogate nuclei of low magnetogyric ratio and to implement heteronuclear correlation spectroscopy. The full potential of the method will unfold when chemical-shift resolution can be introduced because the low-gamma nuclei often show a large chemical-shift dispersion and often also high spectral resolution.

We thank the Schweizerischer Nationalfonds (SNF), the ETH Zurich, and the Kommission für Technologie und Innovation (KTI) for financial support. We acknowledge scientific advice from Dr. Rene Verel and Dr. Matthias Ernst and thank Dr. Bernd Knobloch for drawing our attention to KPF_6.

*Electronic address: beme@ethz.ch

[1] J. A. Sidles, Appl. Phys. Lett. **58**, 2854 (1991).
[2] J. A. Sidles, J. L. Garbini, K. J. Bruland, D. Rugar, O. Zuger, S. Hoen, and C. S. Yannoni, Rev. Mod. Phys. **67**, 249 (1995).
[3] N. Nestle, A. Schaff, and W. S. Veeman, Prog. Nucl. Magn. Reson. Spectrosc. **38**, 1 (2001).
[4] C. L. Degen, Q. Lin, A. Hunkeler, U. Meier, M. Tomaselli, and B. H. Meier, Phys. Rev. Lett. **94**, 207601 (2005).
[5] J. G. Kempf and J. A. Marohn, Phys. Rev. Lett. **90**, 087601 (2003).
[6] J. Jeener, in Proceedings of the Ampere International Summer School, Basko Polje, Jugoslavia, 1971 (unpublished).
[7] W. P. Aue, E. Bartholdi, and R. R. Ernst, J. Chem. Phys. **64**, 2229 (1976).
[8] R. R. Ernst, G. Bodenhausen, and A. Wokaun, *Principles of Nuclear Magnetic Resonance in One and Two Dimensions* (Clarendon Press, Oxford, 1987).
[9] H. J. Mamin, R. Budakian, B. W. Chui, and D. Rugar, Phys. Rev. B **72**, 024413 (2005).
[10] D. Rugar, R. Budakian, H. J. Mamin, and B. W. Chui, Nature (London) **430**, 329 (2004).
[11] R. Verhagen, A. Wittlin, C. W. Hilbers, H. van Kempen, and A. P. M. Kentgens, J. Am. Chem. Soc. **124**, 1588 (2002).
[12] S. R. Hartmann and E. L. Hahn, Phys. Rev. **128**, 2042 (1962).
[13] A. Pines, M. G. Gibby, and J. S. Waugh, J. Chem. Phys. **56**, 1776 (1972).
[14] A. Pines, M. G. Gibby, and J. S. Waugh, J. Chem. Phys. **59**, 569 (1973).
[15] M. Mehring, *Principles of High Resolution NMR in Solids* (Springer, Berlin, 1983), 2nd ed.
[16] D. Rugar, O. Züger, S. Hoen, C. S. Yannoni, H. M. Vieth, and R. D. Kendrick, Science **264**, 1560 (1994).
[17] K. J. Bruland, J. L. Garbini, W. M. Dougherty, and J. A. Sidles, J. Appl. Phys. **80**, 1959 (1996).
[18] C. L. Degen, U. Meier, Q. Lin, A. Hunkeler, and B. H. Meier, Rev. Sci. Instrum. (to be published).
[19] S. Hediger, B. H. Meier, N. D. Kurur, G. Bodenhausen, and R. R. Ernst, Chem. Phys. Lett. **223**, 283 (1994).
[20] G. R. Miller and H. S. Gutowsky, J. Chem. Phys. **39**, 1983 (1963).
[21] The $\omega_1^P/2\pi$ fields were calibrated via the Rabi frequencies of separate nutation experiments.
[22] The fitted CP buildup times are 0.39 and 1.1 ms for the NMR case and MDRFM case, respectively.
[23] $T_1^P = 7.8$ s, $T_{1\rho}^P = 4.7$ s (at $\omega_1^P/2\pi = 7.3$ kHz), $T_1^F = 6.07$ s, $T_{1\rho}^F = 5$ s (at $\omega_1^F/2\pi = 6$ kHz), $T_{1\rho}^P$(MRFM) = $T_{1\rho}^F$(MRFM) = 2.5 s.